Journal of Inorganic Biochemistry 200 (2019) 110801

Contents lists available at ScienceDirect

Journal of Inorganic Biochemistry

journal homepage: www.elsevier.com/locate/jinorgbio

Probing the effect of *N*-alkylation on the molecular recognition abilities of the major groove N7-binding site of purine ligands

María Eugenia García-Rubiño[a], Miquel Barceló-Oliver[b], Alfonso Castiñeiras[c], Alicia Domínguez-Martín[d,*]

[a] Department of Physical Chemistry, Faculty of Pharmacy, University of Granada, 18071 Granada, Spain
[b] Department of Inorganic Chemistry, Faculty of Chemical Science, University of Balearic Island, 07112 Palma, Spain
[c] Department of Inorganic Chemistry, Faculty of Pharmacy, University of Santiago de Compostela, 15782 Santiago de Compostela, Spain
[d] Department of Inorganic Chemistry, Faculty of Pharmacy, University of Granada, 18071 Granada, Spain

A B S T R A C T

The study of the metal binding pattern of *N*-methyladenines (1-, 3-, 7- or 9-Meade) towards Cu^{II}-iminodiacetate-like chelates is addressed on the basis of XRD crystal structures of sixteen novel ternary compounds. Except for three compounds, all others feature an square-based Cu(II) coordination, type 4 + 1, and the efficient cooperation of a Cu−N7 bond with an intra-molecular N6-H···O(coord. carboxylate) interligand interaction as the major metal-binding pattern. The three referred exceptions to this behavior are: (1) the compound $[Cu(MIDA)(7Meade)(H_2O)]\cdot 4H_2O$, which evidence the Cu−N3 binding pattern; the (2) $[Cu(IDA)(1Meade)(H_2O)_2]\cdot 4H_2O$, which molecular recognition consist in the Cu−N9 bond and a (distal aqua)·····N3(1Meade) intra-molecular interaction, within an octahedral Cu(II) center; and (3) $[Cu(IDA)(9Meade)(H_2O)_2]\cdot 3H_2O$, also with a 4 + 1 + 1 Cu(II) coordination, where the Cu−N7 bond exists along with an extremely weak N6-H···O (coord. carboxylate) interaction (3.33 Å, 140.2°). This former interaction is determined by packing forces that promote the participation of the N6−H group in a 'trifurcated' H-bond. In conclusion, the cooperation between the Cu−N7 bond (not possible for 7Meade) and the intra-molecular N6-H···O interaction is clearly favored (a) by the H-accepting role of the O-coordinated carboxylate atoms from the iminodiacetate ligands in *mer*-NO_2 conformation and (b) in compounds where the Cu(II) atom exhibits an elongated square-base pyramidal coordination, type 4 + 1.

1. Introduction

The formation of model mixed-ligand metal complexes having nucleobases, nucleosides or nucleotides as co-ligands is an essential tool that can help us to better understand the interaction between metal ions and nucleic acids and their constituents, and thereby their significance [1,2]. Furthermore, during the last decades, this kind of compounds has also been studied due to their broad interest as molecular models in other areas within the inorganic biochemistry field, such as the study of novel metallo-drugs, metallo-enzymes or the design of metal-organic frameworks (BioMOFs) as delivering systems and the synthesis of novel bio-materials [3–6]. In this context, special attention has been paid to the role of intra- and/or inter-molecular interligand interactions, i.e. both classic and non-conventional H-bonds, π,π-stacking, anion/π or C-H/π interactions, in molecular recognition processes.

Among the natural nucleobases, the extreme coordination versatility of the N-rich ligand adenine (Hade) should be remarked. This versatility is closely related to the borderline Pearson character of all its N-donors but also with the tautomeric possibilities of its neutral and protonated forms [7]. In N-substituted adenines tautomerism is drastically reduced since the tautomeric H-atom (placed on N9 in the most stable Hade tautomer) is missing, hence metal binding patterns of N-substituted adenines are expected to be quite different from Hade. A comprehensive structural search has been carried out in the CSD database for methyladenines (Meade). In this context, a large variety of N9-substituted adenine-like ligands have been reported and studied as simple adenosine models, showing a more restricted coordination chemistry.

The structure of 9Meade has been reported several times, e.g. [8,9], as well as different salts and compounds with the $H(N1)9Meade^+$ cation [10,11] and the dibromide salt of $H_2(N1,N7)9Meade^{2+}$ have been reported [12]. These findings reveal that proton affinity of 9Meade is N1 > N7 > N3, according to the basicity order assumed for Hade (N9 > N1 > N7 > N3). Likewise, crystal structures of different base-pairs with *N*-methyladenines and 1-methyl-pyrididines are also available [13,14]. The known metal binding patterns (MBP) for 9Meade can be summarized as follows: (1) monodentate metal-N7 (Co^{II}, Cu^{II}, Zn^{II}, Ru^{III}, Ag^{I}, Cd^{II}, Os^{II}, Pt^{II}, Hg^{II}, Ir^{III}), e.g. refs. [15-19], (2) monodentate metal-N1 (Hg^{II}, Pt^{II}) [20,21], (3) by monodentate metal-N6 (Pt^{II}, using the rare tautomer H(N1),H(N6)-9Meade) [22], (4) chelating-N6,N7 mode [23] and (5) bridging μ_2-N1,N7 mode (Cu^{II}, Zn^{II}, Ag^{I}, Pt^{II}, and bimetallic compounds with $Pd^{II}(N1)/Pt^{II}(N7)$ or $Ag^{I}(N1)/Pt^{II}(N7)$, e.g.

* Corresponding author at: Department of Inorganic Chemistry, Faculty of Pharmacy, University of Granada, E-18071, Spain.
E-mail address: adominguez@ugr.es (A. Domínguez-Martín).

https://doi.org/10.1016/j.jinorgbio.2019.110801
Received 29 May 2019; Received in revised form 8 August 2019; Accepted 17 August 2019
Available online 19 August 2019
0162-0134/

refs. [18, 19, 24, 25].

In clear contrast, the available structural information about 7Meade is extremely limited. The structure of the neutral 7Meade ligand seems not to be determined. It should be highlighted though the dibromide salt of the H_2(N3,N9)7Meade^{2+} cation [26] and the complex salt H(N3)7Meade[Zn(7Meade)Cl_3] [27] where the complex anion exhibits the bond Zn-N9(7Meade) while the counter-cation is protonated on N3(7Meade). So far, the structure of this latter compound represents the only example of a 7Meade metal derivative! It is striking the general lack of structural information related to N7-subsituted adenines, where only a few ligands have been already described such as 7-benzyl-adenine [28].

The structure of 3Meade remains unknown but not that of close analogues such as 3-ethyladenine [29] or 3-benzyl-adenine [28]. In crystals of the hydrochloride [30] and indole-3-acetate [31] salts, the cation H(N7)3Meade$^+$ is protonated on N7. Hence, the proton affinity in 3Meade could be assumed as N7 > N9 > N1. This is supported by the crystal structure of four mixed-ligand metal complexes which exhibit the monodentate M-N7 metal binding pattern for 3Meade [32–36]. Interestingly, a bridging μ_2-N7,N9 role has also been reported for a CH_3Hg(I) derivative [33]. A unique polymeric complex of Cd(II) exhibits the divalent cation of the peculiar ligand 1-(9H-adenin-1-ium-9-yl)-4-(7H-adenini-3-ium-3-yl)N-butane(2+), [H(N1)9Meade-$(CH_2)_4$-H(N7)3Meade]$^{2+}$ [37]. This result is in agreement to the proton affinities previously described for 9Meade and 3Meade, with both ligands being protonated at their corresponding most basic nitrogen donors: N1 for 9Meade and N7 for 3Meade.

The crystal structure of 1Meade is not reported but it is known that of 1-(2-isopentenyl)adenine [38]. The crystal structures of two chloride salts of 1Meade evidence the presence of the H(N9)1Meade$^+$ and H_2(N7,N9)1Meade^{2+} cations [39], thus suggesting the N9 > N7 > N3 proton affinity order for 1Meade. Moreover, Sheldrick et al. proved that in the compound [MeHg(1Meade)(NO_3)] metallation occurs on N9, as well as the ability of 1Meade to play the μ_3-N3,N7,N9 role with MeHg$^+$ ions [39].

Over the past decades, our research group has been devoted to studying mixed-ligand copper(II) complexes involving purine-like ligands. In this context, the current work aims to unravel how the presence of non-coordinating N-R arms, both in the chelator and the N-ligand, influences the molecular recognition pattern between different Cu(II) chelates and N(heterocyclic)-methyladenine derivatives (1Meade, 3Meade, 7Meade or 9Meade). To this purpose the iminodiacetate chelator as well as several iminodiacetate derivatives have been studied (Scheme 1). Special attention will be also paid to weak intra- and intermolecular interactions that might drive the metal binding pattern.

2. Experimental

2.1. Reagents

Bluish $Cu_2CO_3(OH)_2$ was purchased from Probus. Iminodiacetic acid (IDA), *N*-methyliminodiacetic acid (H_2MIDA), 1-methyladenine, 3-methyladenine, 7-methyladenine and 9-methyladenine were supplied by Sigma-Aldrich. All reagents were used as received. *N*-ethyl-, *N*-benzyl-, *N*-(*p*-methylbenzyl)-, *N*-(p-chlorobenzyl)-, *N*-furfuryl- and *N*-(1-naphtyl-methyl)iminodiacetic acids (H_2EIDA, H_2NBzIDA, H_2MEBIDA and H_2CBIDA, H_2FurIDA and H_2NamIDA, respectively) were synthesised in their acid form as reported in Refs. [40-42].

2.2. Syntheses of novel metal complexes

A similar synthetic procedure was used for all the reported compounds, therefore a general procedure will be first described and then information about each of the compounds will be detailed.

2.3. Synthesis

2.3.1. General synthetic procedure

In a Kitasato flask, $Cu_2CO_3(OH)_2$ (0.25 mmol) was reacted with 0.5 mmol of the corresponding iminodiacetic-like acids H_2IDA (**1**,**4**,**11**), H_2MIDA (**5**,**10**,**12**), H_2EIDA (**13**), H_2FurIDA (**8**), H_2NBzIDA (**6**,**14**), H_2MEBIDA (**15**), H_2CBIDA (**2**,**9**,**16**) and H_2NamIDA (**3**,**7**) in 60 mL of distilled water with heating (50 °C), stirring and moderate vacuum. Once a clear blue solution of the binary chelate was obtained, the corresponding Meade ligand (0.5 mmol) was added: 1Meade (**1**–**3**), 3Meade (**4**–**9**), 7Meade (**10**), 9Meade (**11**–**16**). The solution was left reacting for one hour. Afterwards, it was filtered in a crystallization device (to remove possible un-reacted materials) and stood at r.t. covered with a plastic film to control the evaporation of the solvents.

*2.3.1.1. [Cu(IDA)(1Meade)(H_2O)$_2$]·4H_2O (**1**).* In one week, very thing needle-like blue crystals started to appear. Crystals were allowed to grow during one moth and then collected for X-ray diffraction (XRD) purposes. Yield ca. 55%. Elemental analysis (%): Calc. for $C_{10}H_{26}CuN_6O_{11}$ (**1**) C 25.56, H 5.58, N 17.89; Found: C 25.53H 5.48 N 17.84. FT-IR [KBr, cm^{-1}]: $\upsilon_{as}(H_2O)$ 3444, $\upsilon_s(H_2O)$ 3257, $\upsilon_{as}(NH_2)$ overshadowed, $\upsilon_s(NH_2)$ 3225, $\upsilon_{as}(CH_3)$ 2967, $\upsilon_d(CH_3)$ 2851, $\delta(NH_2)$ 1646, $\delta(H_2O)$ and υ_{as}(COO) overlapped 1615, υ_s(COO) 1383, $\pi(C-H)_{ar}$ (1MeAde) 783. The thermo-gravimetric curve is divided in four steps. The UV–Vis spectrum shows an asymmetric d-d band with λ_{max} at 709 nm (ν_{max} 14,104 cm^{-1}). Under air-dry flow, the compound losses almost all the non-coordinated water. The amount of remaining water after this point varies depending on the sample grinding, leading to slightly different TG starting points. In all cases, during the first step (from 20 to 70 °C), the remaining water is lost with good agreement between calculated and experimental values (e.g. n = 0.07, Calc. 0.347%; Found 0.320%). During the pyrolysis of the organic ligands H_2O, CO_2, CO, N-oxide gases (N_2O, NO and NO_2), as well as, traces amounts of ammonia, are evolved, yielding a final CuO·$Cu(OH)_2$ residue (460 °C, Calc. 48.78; Found 47.22%).

*2.3.1.2. [Cu(CBIDA)(1Meade)(H_2O)]·3H_2O (**2**).* In four months, suitable needle-like blue crystals were collected for XRD purposes. Yield ca. 75%. Elemental analysis (%) Calc. for $C_{17}H_{25}ClCuN_6O_8$ (**1**) C 37.78, H 4.66, N 15.55; Found: C 37.85H 4.52 N 15.57. FT-IR [KBr, cm^{-1}]: $\upsilon_{as}(H_2O)$ 3387, $\upsilon_{as}(NH_2)$ and $\upsilon_s(H_2O)$ 3292, $\upsilon_s(NH_2)$ 3123, $\upsilon_{as}(CH_3)$ 2970, $\upsilon_d(CH_3)$ 2851, $\upsilon_{as}(CH_2)$ 2924, $\upsilon_s(CH_2)$ 2828, $\delta(NH_2)$ and $\delta(H_2O)$ overlapped 1624, υ_{as}(COO) 1563, υ_s(COO) 1384, $\pi(C-H)_{ar}$ (1MeAde) 786, $\pi(C-H)_{ar}$ (CBIDA) 643. The UV–Vis spectrum shows an asymmetric d-d band with λ_{max} at 702 nm (ν_{max} 14,245 cm^{-1}). The thermo-gravimetric curve is divided in five steps. Under air-dry flow, the compound losses almost all the non-coordinated water. Hence, the TG experiment starts with an average formula [Cu(CBIDA)(1MeAde)(H_2O)]·0.5H_2O. In the first step (from 20 to 120 °C), 0.5 solvent molecule plus the apical aqua ligand are lost (n = 1.5, Calc. 5.455%; Found 6.937%). During the pyrolysis of the organic ligands H_2O, CO_2, CO, N-oxide gases (N_2O, NO and NO_2), as well as, peculiarly, isocyanid acid, are evolved. This yields a final CuO residue (640 °C, Calc. 16.057; Found 18.216%).

*2.3.1.3. [Cu(NamIDA)(1MeadeH)Cl]·5H_2O (**3**).* The presence of chloride ions in this compound are attributed to an error during the synthesis, most probably related to the use of the water pump, which allowed chloride ions to get in the solution. No suitable crystals for XRD were directly isolated from this synthesis, thus the obtained crystals were again dissolved in water and grown under ether diffusion. After one month, suitable blue crystals were collected for XRD purposes. Yield ca. 45%. Elemental analysis (%) Calc. for $C_{21}H_{31}ClCuN_6O_9$ (**1**) C 41.31, H 5.12, N 13.77; Found: C 41.28H 5.12 N 13.73. FT-IR [KBr, cm^{-1}]: $\upsilon_{as}(H_2O)$ 3397, $\upsilon_{as}(NH_2)$ and $\upsilon_s(H_2O)$ overshadowed, $\upsilon_s(NH_2)$ 3194, $\upsilon_{as}(CH_3)$ 2981, $\upsilon_d(CH_3)$ 2851, $\upsilon_{as}(CH_2)$ 2926, $\upsilon_s(CH_2)$ 2856,

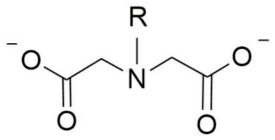

Iminodiacetate-like(2-) anion

R = H (IDA)
R = -CH_3 (MIDA)
R = -CH_2-CH_3 (EIDA)
R = -Furfuryl (FurIDA)
R = -CH_2-Ph (NBzIDA)
R = -CH_2-Ph-CH_3 (MEBIDA)
R = -CH_2-Ph-Cl (CBIDA)
R = -1-naphtylmethyl (NamIDA)

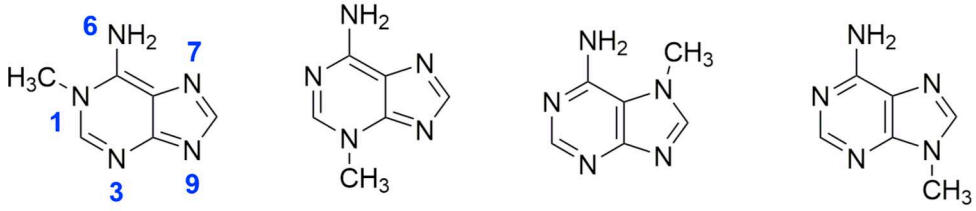

1Meade 3Meade 7Meade 9Meade

Scheme 1. Top, iminodiacetate-like(2-) chelators used in this work. Bottom, *N*-methyladenines used in this work: 1-methyladenine (1Meade), 3-methyladenine (3Meade), 7-methyladenine (7Meade) and 9-methyladenine (9Meade). Conventional purine notation number has been specified on 1Meade ligand.

$\delta(NH_2)$ and $\delta(H_2O)$ overlapped 1618, $\upsilon_{as}(COO)$ 1596, $\upsilon_s(COO)$ 1384, $\pi(C{-}H)_{ar}$ (1MeAde) 790. The UV–Vis spectrum shows an asymmetric d-d band with λ_{max} at 653 nm (ν_{max} 15,315 cm^{-1}). The thermo-gravimetric curve is divided in five steps. Under air-dry flow, the compound losses part of the solvent water, therefore the TG experiment starts with an average formula [Cu(NamIDA)(1MeAdeH)Cl]·2.4 H_2O. In the first step (from 20 to 145 °C), the remaining water molecules are lost (n = 2.4, Calc. 7.670%; Found 7.627%). During the pyrolysis of the organic ligands H_2O, CO_2, CO, NH_3 and N-oxide gases (N_2O, NO and NO_2) are evolved. This yields a final CuO residue (640 °C, Calc. 14.112; Found 16.096%).

*2.3.1.4. [Cu(IDA)(3Meade)(H_2O)$_2$]·3H_2O (**4**).* In four weeks, parallelepiped greenish crystals were isolated from the mother solution and studied by XRD. In addition, crystals of the binary chelate [Cu(IDA)(H_2O)$_2$] and free 3Meade were collected. The nature of these latter crystals was confirmed by FT-IR. Yield ca. 63%. Elemental analysis (%): Calc. for $C_{10}H_{22}CuN_6O_9$ (**2**) C 27.68, H 5.11, N 19.37; Found: C 27.76, H 5.23, N 19.30. FT-IR [KBr, cm^{-1}]: $\upsilon_{as}(H_2O)$ 3414, $\upsilon_{as}(NH_2)$ 3302, $\upsilon_s(H_2O)$ and $\upsilon_s(NH_2)$ overlapped 3245, $\upsilon(N{-}H)$ 3144, $\upsilon_{as}(CH_3)$ 2949, $\upsilon_d(CH_3)$ overshadowed, $\upsilon_{as}(CH_2)$ 2943, $\upsilon_s(CH_2)$ 2848, $\delta(NH_2)$ 1660, $\delta(H_2O)$ and $\upsilon_{as}(COO)$ overlapped 1615, $\delta(N{-}H)$ 1522, $\upsilon_s(COO)$ 1384, $\pi(C{-}H)_{ar}$ (3MeAde) 813. The UV–Vis spectrum shows an asymmetric d-d band with λ_{max} at 732 nm (ν_{max} 13,661 cm^{-1}). The thermo-gravimetric curve is divided in five steps. Under air-dry flow, the compound losses part of the solvent molecules. Hence, the TG experiment starts with an average formula [Cu(IDA)(3MeAde)(H_2O)$_2$] ·0.9H_2O. In the first step (from 30 to 180 °C), 0.9 water molecules plus the two apical aqua ligands in the 4 + 1 + 1 Cu (II) surrounding are lost (n = 2.9, Calc. 13.192%; Found 13.860%). During the pyrolysis of the organic ligands, H_2O, CO_2, CO, trimethylamine (TMA), NH_3, N_2O, NO and NO_2 gases were evolved, yielding to a CuO residue (530 °C, Calc. 20.086%; Found 21.837%).

*2.3.1.5. [Cu(MIDA)(3Meade)(H_2O)]·6H_2O (**5**).* After six weeks, suitable parallelepiped blue crystals were collected for XRD purposes. Yield ca. 85%. Elemental analysis (%): Calc. for $C_{11}H_{28}CuN_6O_{11}$ (**3**) C 27.30, H 5.83, N 17.37; Found: C 27.42, H 5.79, N 17.30. FT-IR [KBr, cm^{-1}]: $\upsilon_{as}(H_2O)$ 3433, $\upsilon_{as}(NH_2)$ 3332, $\upsilon_s(H_2O)$ 3240, $\upsilon_s(NH_2)$ 3118, two types of $\upsilon_{as}(CH_3)$ 3112 and 2968, $\upsilon_d(CH_3)$ overshadowed, $\upsilon_{as}(CH_2)$ 2937, $\upsilon_s(CH_2)$ 2855, $\delta(NH_2)$ 1668, $\delta(H_2O)$ and $\upsilon_{as}(COO)$ overlapped 1618, $\upsilon_s(COO)$ 1384, $\pi(C{-}H)_{ar}$ (3MeAde) 809. The UV–Vis spectrum shows an asymmetric d-d band with λ_{max} at 714 nm (ν_{max} 14,006 cm^{-1}). The thermal behaviour of this compound is divided in five steps. Under air-dry flow, the sample loses four solvent molecules, thus the TG experiment starts with an average formula [Cu(MIDA)(3Meade)(H_2O)]·H_2O. In the two first steps, from 30 to 175 °C, the compound only loses water according to the recorded evolved gases. Thus, the first step corresponds to the loss of the non-coordinated water molecule (n = 1, Calc. 4.794%; Found 4.887%) and the second step corresponds to the loss of the apical aqua ligand (n = 1, Calc. 4.355%; Found 4.243%). The consecutive pyrolytic steps (from 175 to 490 °C) yield to a CuO residue (Calc. 21.165%, Found 22.311%). The evolved gases during the pyrolysis are H_2O, CO_2, CO, TMA, NH_3 and N-oxide gases (N_2O, NO and NO $_2$). TMA is typically observed from the pyrolysis of MIDA chelating ligand.

*2.3.1.6. [Cu(NBzIDA)(3Meade)(H_2O)]·2H_2O (**6**).* After six weeks, parallelepiped blue crystals appeared, suitable for XRD. Yield of this synthesis is approx. 85%. Elemental analysis (%): Calc. for $C_{17}H_{24}CuN_6O_7$ (**4**) C 41.84, H 4.96, N 17.22; Found: C 41.80, H 5.00, N 17.29. FT-IR [KBr, cm^{-1}]: $\upsilon_{as}(H_2O)$ 3425, $\upsilon_{as}(NH_2)$ overshadowed, $\upsilon_s(H_2O)$ 3291, $\upsilon_s(NH_2)$ 3166, $\upsilon_{as}(CH_3)$ 2980, $\upsilon_d(CH_3)$ 2889, $\upsilon_{as}(CH_2)$ 2928, $\upsilon_s(CH_2)$ 2871, $\delta(NH_2)$ and $\delta(H_2O)$ overlapped 1612, $\upsilon_{as}(COO)$ 1595, $\upsilon_s(COO)$ 1384, $\pi(C{-}H)_{ar}$ (3Meade) 805, $\pi(C{-}H)_{ar}$ (NBzIDA) 712. The UV–Vis spectrum shows an asymmetric d-d band with λ_{max} at 737 nm (ν_{max} 13,569 cm^{-1}). The thermal behaviour is divided in six steps. Under air-dry flow, the sample loses the non-coordinated water. Afterwards, the sample [Cu(NBzIDA)(3Meade)(H_2O)$_{0.8}$] experiments the loss of weight of the apical aqua ligand (30–125 °C; Calc. 3.215%; Found: 3.550%). Five additional pyrolytic steps produce as evolved gases H_2O, CO_2, CO (t) N-oxide gases (N_2O, NO, NO_2) to yield an impure CuO residue at 545 °C (Calc. 17.743%; Found 19.148%).

*2.3.1.7. [Cu(NamIDA)(3Meade)(H_2O)]·2H_2O (**7**).* The obtained solution precipitates after the addition of 3Meade, then the solution was filtered and the precipitate re-dissolved in a 1:1 water:methanol mixture. After three weeks, fine turquoise crystals appeared, suitable

for XRD. Yield of this synthesis is approx. 80%. Elemental analysis (%): Calc. for $C_{17}H_{24}CuN_6O_7$ (**4**) C 46.88, H 4.87, N 15.62; Found: C 46.80, H 5.00, N 15.59. FT-IR [KBr, cm^{-1}]: $\upsilon_{as}(H_2O)$ 3420, $\upsilon_{as}(NH_2)$ 3345, $\upsilon_s(H_2O)$ 3238, $\upsilon_s(NH_2)$ 3207, $\upsilon_{as}(CH_3)$ 2961, $\upsilon_d(CH_3)$ 2930, $\delta(NH_2)$ and $\delta(H_2O)$ overlapped 1627, $\upsilon_{as}(COO)$ 1595, $\upsilon_s(COO)$ 1361, $\pi(C-H)_{ar}$ (3Meade) 810. The UV–Vis spectrum shows an asymmetric d-d band with λ_{max} at 684 nm (ν_{max} 14,620 cm^{-1}). The thermal behaviour is divided in four steps. Under air-dry flow, the sample loses almost all the non-coordinated water molecules, leading to the following starting TG formula [Cu(NamIDA)(3Meade)(H_2O)]·0.2H_2O. In the first step, the loss of weight of the apical aqua ligand plus the remaining solvent water was observed (30–170 °C; Calc. 6.279%; Found: 6.290%). Three additional pyrolytic steps produce as evolved gases H_2O, CO_2, CO, NH_3 and N-oxide gases (N_2O, NO, NO_2) to yield an impure CuO residue at 545 °C (Calc. 15.404%; Found 16.643%).

*2.3.1.8. [Cu(FurIDA)(3Meade)(H_2O)]·4H_2O (**8**)*. After five weeks, parallelepiped blue crystals appeared, suitable for XRD. Yield of this synthesis is approx. 80%. Elemental analysis (%): Calc. for $C_{15}H_{26}CuN_6O_{10}$ (**4**) C 35.05, H 5.10, N 16.35; Found: C 35.12, H 5.00, N 16.38. FT-IR [KBr, cm^{-1}]: $\upsilon_{as}(H_2O)$ 3446, $\upsilon_{as}(NH_2)$ 3351, $\upsilon_s(H_2O)$ 3237, $\upsilon_s(NH_2)$ 3125, $\upsilon_{as}(CH_3)$ 2955, $\upsilon_d(CH_3)$ 2930, $\upsilon_{as}(CH_2)$ overshadowed, $\upsilon_s(CH_2)$ 2855, $\delta(NH_2)$ and $\delta(H_2O)$ overlapped 1620, $\upsilon_{as}(COO)$ overshadowed, $\upsilon_s(COO)$ 1385, $\pi(C-H)_{ar}$ (3Meade) 808, $\pi(C-H)_{ar}$ (3H-FurIDA) 781. The thermal behaviour is divided in five steps. Under air-dry flow, the sample loses almost all the non-coordinated water molecules, leading to the following starting TG formula [Cu(FurIDA)(3Meade)(H_2O)]·0.64H_2O. The loss of weight of the remaining water molecules is observed along the two first steps (30–260 °C; Calc. 6.785%; Found: 6.650%). Three additional pyrolytic steps produce as evolved gases H_2O, CO_2, CO, CH_4, NH_3 and N-oxide gases (N_2O, NO, NO_2) to yield a CuO residue at 550 °C (Calc. 18.268%; Found 18.705%).

*2.3.1.9. {[Cu(CBIDA)(3Meade)]·H_2O}$_n$ (**9**)*. After four weeks, bad shaped blue crystals appeared, not suitable for XRD. Further re-crystallizations in 1:1 water:isopropanol mixtures finally yield to parallelepiped crystals appropriate for XRD purposes. Yield ca. 15%. Elemental analysis (%): Calc. for $C_{17}H_{23}ClCuN_6O_7$ (**5**) C 39.09, H 4.44, N 16.09; Found: C 38.97, H 4.35, N 16.15. FT-IR [KBr, cm^{-1}]: $\upsilon_{as}(H_2O)$ 3436, $\upsilon_{as}(NH_2)$ 3336, $\upsilon_s(H_2O)$ 3232, $\upsilon_s(NH_2)$ 3167, $\upsilon_{as}(CH_3)$ 2960, $\upsilon_d(CH_3)$ 2881, $\upsilon_{as}(CH_2)$ 2936, $\upsilon_s(CH_2)$ 2851, $\delta(NH_2)$ 1635, $\delta(H_2O)$ 1611, $\upsilon_{as}(COO)$ 1604, $\upsilon_s(COO)$ 1384, $\pi(C-H)_{ar}$ (3Meade) 805, $\pi(C-H)_{ar}$ (CBIDA) 645. Further UV–Vis and thermo-gravimetric analyses were not performed since it was not possible to have enough pure samples.

*2.3.1.10. [Cu(MIDA)(7Meade)(H_2O)·4H_2O (**10**)*. In two months, small parallelepiped blue crystals appeared. After several re-crystallizations, the size of the crystals slightly improves and XDR analyses were performed. Yield of this synthesis is approx. 15%. Elemental analysis (%): Calc. for $C_{11}H_{24}CuN_6O_9$ (**5**) C 29.50, H 5.40, N 18.79; Found: C 29.64, H 5.32, N 18.60. FT-IR [KBr, cm^{-1}]: $\upsilon_{as}(H_2O)$ 3402, $\upsilon_{as}(NH_2)$ 3340, $\upsilon_s(H_2O)$ and $\upsilon_s(NH_2)$ overlapped 3232, $\upsilon_{as}(CH_3)$ 2973, $\upsilon_d(CH_3)$ 2857, $\upsilon_{as}(CH_2)$ 2927, $\upsilon_s(CH_2)$ 2825, $\delta(NH_2)$, $\delta(H_2O)$ and $\upsilon_{as}(COO)$ overlapped 1640, $\upsilon_s(COO)$ 1374, $\pi(C-H)_{ar}$ (7Meade) 789. UV–Vis and thermogravimetric analyses were not performed since it was not possible to have enough pure crystalline sample.

*2.3.1.11. [Cu(IDA)(9Meade)(H_2O)$_2$]·3H_2O (**11**)*. In two weeks, needle-like blue crystals were collected for XRD purposes. Yield is ca. 80–85%. Elemental analysis (%): Calc. for $C_{10}H_{22}CuN_6O_9$ (**6**) C 27.68, H 5.11, N 19.37; Found: C 27.73, H 4.99, N 19.35. FT-IR [KBr, cm^{-1}]: $\upsilon_{as}(H_2O)$ 3419, $\upsilon_{as}(NH_2)$ 3337, $\upsilon_s(H_2O)$ and $\upsilon_s(NH_2)$ overlapped 3238, υ (N—H) overshadowed, $\upsilon_{as}(CH_3)$ 2965, $\upsilon_d(CH_3)$ overshadowed, $\upsilon_{as}(CH_2)$ 2934, $\upsilon_s(CH_2)$ 2858, $\delta(NH_2)$ 1653, $\delta(H_2O)$ 1620, δ(N—H) overshadowed, $\upsilon_{as}(COO)$ 1599, $\upsilon_s(COO)$ 1385, $\pi(C-H)_{ar}$ (9MeAde) 791. The UV–Vis spectrum shows an asymmetric d-d band with λ_{max} at 713 nm (ν_{max} 14,025 cm^{-1}). The thermo-gravimetric curve is divided in five steps. Under air-dry flow, the sample losses nearly all the non-coordinated water molecules. Hence, the starting sample for the TG experiment agree to the formula [Cu(IDA)(9Meade)(H_2O)$_2$]·0.4H_2O. The 0.4 water molecules as well as the two apical aqua ligands, in the 4 + 1 + 1 Cu (II) surrounding, are lost during the first step (n = 2.4, Calc. 11.172%; Found 11.661%). Consecutive steps are assigned to the pyrolysis of the organic ligands. FT-IR spectra of the evolved gasses show H_2O, CO_2, CO, NH_3, TMA(t), as well as N-oxide gases (N_2O, NO and NO_2). Finally, it yields to a CuO residue at 530 °C (Calc. 20.553%; Found 21.543%).

*2.3.1.12. {[Cu(MIDA)(9Meade)(H_2O)]·2H_2O}$_n$ (**12**)*. After six weeks, well-shaped parallelepiped blue crystals appeared, suitable for XRD purposes. Typical yield of this synthesis is ca. 80–85%. Elemental analysis (%): Calc. for $C_{11}H_{20}CuN_6O_7$ (**7**) C 32.08, H 4.89, N 20.41; Found: C 32.12, H 4.96, N 20.36. FT-IR [KBr, cm^{-1}]: $\upsilon_{as}(H_2O)$ 3452, $\upsilon_{as}(NH_2)$ 3380, $\upsilon_s(H_2O)$ 3182, $\upsilon_s(NH_2)$ 3136, $\upsilon_{as}(CH_3)$ 2977, $\upsilon_d(CH_3)$ 2861, $\upsilon_{as}(CH_2)$ 2932, $\upsilon_s(CH_2)$ 2859, $\delta(NH_2)$ and $\delta(H_2O)$ overlapped 1635, $\upsilon_{as}(COO)$ 1601, two types of $\upsilon_s(COO)$ 1396 and 1384, $\pi(C-H)_{ar}$ (9MeAde) 793. The UV–Vis spectrum shows an asymmetric d-d band with λ_{max} at 697 nm (ν_{max} 14,347 cm^{-1}). The thermal behaviour of this compound is divided in four steps. Under air-dry flow, the sample loses all the solvent molecules and part of the apical aqua ligand, thus the TG experiment starts with an average formula [Cu(MIDA)(9Meade)(H_2O)$_{0.8}$]. In the first step, the compound loses the rest of the remaining aqua (n = 0.8; Calc. 3.872%, Found 3.520%). Then, consecutive pyrolytic steps (from 170 to 490 °C) yield to a CuO residue (Calc. 21.370%, Found 22.253%). The evolved gases during the pyrolysis are H_2O, CO_2, CO, CH_4, TMA, NH_3 and N-oxide gases (N_2O, NO and NO $_2$). TMA is found in the second step and is typically observed from pyrolysis of MIDA chelating ligand.

*2.3.1.13. {[Cu(EIDA)(9Meade)]·4H_2O}$_n$ (**13**)*. In four months, suitable needle-like blue crystals were collected for XRD purposes. Yield of the synthesis ca. 70–75%. Elemental analysis (%): Calc. for $C_{12}H_{24}CuN_6O_8$ (**8**) C 32.47, H 5.45, N 18.93; Found: C 32.50, H 5.13, N 18.88. FT-IR [KBr, cm^{-1}]: $\upsilon_{as}(H_2O)$ 3441, $\upsilon_{as}(NH_2)$ 3356, $\upsilon_s(H_2O)$ and $\upsilon_s(NH_2)$ overlapped 3185, $\upsilon_{as}(CH_3)$ 2981, $\upsilon_d(CH_3)$ 2877, $\upsilon_{as}(CH_2)$ 2940, $\upsilon_s(CH_2)$ overshadowed, $\delta(NH_2)$ and $\delta(H_2O)$ 1624 overlapped, $\upsilon_{as}(COO)$ 1606, two types of $\upsilon_s(COO)$ 1385 and 1394, $\pi(C-H)_{ar}$ (9Meade) 793. The UV–Vis spectrum shows an asymmetric d-d band with λ_{max} at 671 nm (ν_{max} 14,903 cm^{-1}). The sample losses nearly 40% of the water content under air-dry flow, thus the starting sample for the thermo-gravimetric experiment agree to the formula {[Cu(EIDA) (9Meade)]·1.5H_2O}$_n$. The remaining non-coordinated water is lost during the first step (30–160 °C; Calc. 6.775%; Found 6.393%). The following pyrolytic steps lead to the decomposition of the sample producing H_2O, CO_2, CO, CH_4, NH_3 and N-oxide gases (N_2O, NO, NO_2) to yield, at 540 °C, a final CuO residue (Calc. 19.942%; Found 20.723%).

*2.3.1.14. [Cu(NBzIDA)(9MeAde)(H_2O)]·4H_2O (**14**)*. In two weeks, parallelepiped greenish crystals appeared, suitable for XRD purposes. Typical yield of this synthesis is ca. 90%. Elemental analysis (%): Calc. for $C_{17}H_{28}CuN_6O_9$ (**9**) C 38.97, H 5.39, N 16.04; Found C 38.56, H 5.00, N 16.34. FT-IR [KBr, cm^{-1}]: $\upsilon_{as}(H_2O)$ 3389, $\upsilon_{as}(NH_2)$ overshadowed, $\upsilon_s(H_2O)$ and $\upsilon_s(NH_2)$ overlapped 3197, $\upsilon_{as}(CH_3)$ 2962, $\upsilon_d(CH_3)$ 2847, $\upsilon_{as}(CH_2)$ overshadowed, $\upsilon_s(CH_2)$ overshadowed, $\delta(NH_2)$ and $\delta(H_2O)$ overlapped 1621, $\upsilon_{as}(COO)$ 1597, $\upsilon_s(COO)$ 1384, $\pi(C-H)_{ar}$ (9Meade) 795, $\pi(C-H)_{ar}$ (NBzIDA) 716. The UV–Vis spectrum shows an asymmetric d-d band with λ_{max} at 748 nm(ν_{max} 13,369 cm^{-1}). The thermo-gravimetric curve is divided in four steps. Under air-dry flow, the sample losses part of the solvent molecules, thus the TG experiment starts with an average formula [Cu(NBzIDA)(9Meade) (H_2O)]·0.9H_2O. The 0.9 water molecules as well as the apical aqua ligand, in the 4 + 1

Cu(II) surrounding, are lost during the first step (n = 1.9, Calc. 7.099%; Found 7.245%). This is in accordance with the recorded evolved gases during such step where only H_2O was identified. In the following pyrolytic steps (from 110 to 545 °C), the sample is decomposed producing H_2O, CO_2, CO and N-oxide gases (N_2O, NO, NO_2) to yield a final CuO residue within the experimental error (Calc. 16.497%; Found 17.888%).

*2.3.1.15. [Cu(MEBIDA)(9MeAde)(H$_2$O)]·3H$_2$O (**15**).* In three weeks, parallelepiped greenish crystals appeared, suitable for XRD purposes. Yield ca. 90%. Elemental Analysis (%): Calc. for $C_{18}H_{28}CuN_6O_8$ (**10**), C 41.58, H 5.43, N 16.16; Found C 41.64, H 5.40, N 16.05. FT-IR [KBr, cm^{-1}]: $\upsilon_{as}(H_2O)$ 3369, $\upsilon_{as}(NH_2)$ overshadowed, $\upsilon_s(H_2O)$ and $\upsilon_s(NH_2)$ 3184 overlapped, two types of $\upsilon_{as}(CH_3)$ 2981 and 2967, $\upsilon_d(CH_3)$ 2860, $\upsilon_{as}(CH_2)$ 2922, $\upsilon_s(CH_2)$ overshadowed, $\delta(NH_2)$ and $\delta(H_2O)$ overlapped 1620, $\upsilon_{as}(COO)$ 1597, $\upsilon_s(COO)$ 1384, $\pi(C-H)_{ar}$ (9MeAde) 795, $\pi(C-H)_{ar}$ (MEBIDA) 807. The UV–Vis spectrum shows an asymmetric d-d band with λ_{max} at 738 nm (ν_{max} 13,550 cm^{-1}). The thermal behaviour of **2** is divided in five steps. Under air-dry flow, the sample losses almost all the non-coordinated water. Hence the TG experiment starts with an average formula [Cu(MEBIDA)(9Meade)(H_2O)]·0.7H_2O. In the first step, the sample experiments the loss of 1.7 water molecules (Calc. 6.593%; Found 6.390%). Then, consecutive steps are assigned to the pyrolysis of the organic ligands. FT-IR spectra of the evolved gasses show H_2O, CO_2, CO, CH_4 plus N-oxide gases such as N_2O, NO and NO_2. Finally, it yields to a CuO residue (550 °C; Calc. 16.497%; Found 17.888%).

*2.3.1.16. [Cu(CBIDA)(9Meade)(H$_2$O)]·H$_2$O (**16**).* In one month, very thing needle-like crystals appeared, not suitable for XRD purposes. Such solution was filtered several times in an attempt to improve the size of the crystals. After two months, some parallelepiped blue crystals appeared although it was impossible to isolate good quality ones. Therefore, a new strategy of synthesis was followed: to a new 50 mL solution the aforementioned binary chelate [$Cu_2CO_3(OH)_2$ (0.25 mmol, 0.055 g) + H_2CBIDA acid (0.5 mmol, 0.129 g)], a 40 mL solution of the base pair 9Meade:Thymine (0.5 mmol, 0.074 g: 0.063 g) was added. The reacting mixture was stirred for 12 h at room temperature. After one month, good shape parallelepiped crystals were collected for XRD purposes with a yield of 30–35%. One month later, crystals of free thymine, free 9Meade and the above-mentioned needle-like blue crystals appeared. The former free ligands were identified by FT-IR spectroscopy. The two kind of blue crystals (parallelepiped and needle-like) were characterized by elemental analysis, thermo-gravimetry and FT-IR spectroscopy. Moreover, UV–Vis and XRD was only carried out for the parallelepiped blue crystals. (i) Parallelepiped crystals: Elem. Anal. (%) for $C_{17}H_{21}ClCuN_6O_6$ (**11**) Calc. C 40.48, H 4.20, N 16.66; Found C 38.15, H 5.35, N 16.20. FT-IR (KBr) cm^{-1}: $\upsilon_{as}(H_2O)$ 3435, $\upsilon_{as}(NH_2)$ 3369, $\upsilon_s(H_2O)$ 3250 (sh), $\upsilon_s(NH_2)$ 3192, $\upsilon_{as}(CH_3)$ 2977, $\upsilon_d(CH_3)$ 2853, $\upsilon_{as}(CH_2)$ 2927, $\upsilon_s(CH_2)$ 2846, $\delta(NH_2)$ and $\delta(H_2O)$ overlapped 1623, $\upsilon_{as}(COO)$ 1596, $\upsilon_s(COO)$ 1385, $\pi(C-H)_{ar}$ (9Meade) 795, $\pi(C-H)_{ar}$ (CBIDA) 641. The UV–Vis spectrum shows an asymmetric d-d band with υ_{max} at 14306 cm^{-1}. The thermo-gravimetric curve shows four steps. Under dry-air flow, the sample remains stable so that is in the first step when the two water molecules are lost (n = 2, Calc. 7.143%; Found 6.9715), according to the evolved gasses. The three following steps (from 170 °c to 760 °C) concern the pyrolysis of the dehydrated compound [Cu(CBIDA)(9MeAde)]. Herein, the H_2O, CO_2, CO, CH_4 and N-oxide gases (N_2O, NO, NO_2) were identified. A residue of CuO was found at 760 °C within the experimental error (Calc. 15.770%; Found 14.882%). (ii) Needle-like crystals: Elem. Anal. (%): Calc. for $C_{28}H_{27}Cl_2Cu_2N_7O_8$ (12) Calc. C 34.75, H 4.90, N 10.13; Found C 34.78, H 5.02, N 10.03. These data is in accordance to a formula type [Cu_2(CBIDA)$_2$(μ_2-9Meade)(H_2O)$_2$]·8H_2O. Considering that the same chromophores would be present in both samples, no relevant differences are found between FT-IR of parallelepiped and needle-like crystals. However, it should be noted that those bands related with water are significantly broaden in the latter compound, what is in agreement with our proposed formula. Likewise, the thermo-gravimetric analysis of the needle-like crystals is in line with higher water content. In this case, the compound would lose the major part of the water content under dry-air flow, starting the TG experiment with a formula [Cu_2(CBIDA)$_2$(μ_2-9Meade)(H_2O)$_2$]·0.5H_2O. Thus, the first step of the thermo-gravimetric curve agrees to the loss of 2.5 water molecules (from 20 to 160 °C; n = 2.5 Calc. 5.409%; Found 5.060%). A slightly different decomposition for this compound is evidenced by the gases evolved during the pyrolysis: H_2O, CO_2, CO, CHO and N-oxide gases (N_2O, NO, NO_2). The pyrolysis of the ligand yields to an impure residue of CuO. Further attempts to crystallize the expected compound [Cu_2(CBIDA)$_2$(μ_2-9Meade)(H_2O)$_2$]·8H_2O have not been successful.

2.4. Crystallographic methods

Measured crystals were prepared under inert conditions immersed in perfluoropolyether as protecting oil for manipulation. Suitable crystals were mounted on MiTeGen Micromounts™ and these samples were used for data collection. Data were collected with Bruker SMART APEX (**1–3**,**8**,**13–16**, 293 K), Bruker X8 KappaAPEXII (**4–7**,**8–11**, 100 K) diffractometers. The data were processed with APEX2 program [43] and corrected for absorption using SADABS [44]. The structures were solved by direct methods [45], which revealed the position of all non-hydrogen atoms. These atoms were refined on F^2 by a full-matrix least-squares procedure using anisotropic displacement parameters [45]. All hydrogen atoms were located in difference Fourier maps and included as fixed contributions riding on attached atoms with isotropic thermal displacement parameters 1.2 times those of the respective atom. Geometric calculations were carried out with PLATON [46] and drawings were produced with PLATON [46] and MERCURY [47]. Crystallographic data for the structural analysis have been deposited in the Cambridge Crystallographic Data Centre with numbers 1,919,112–1,919,127, with 1,919,112 corresponding to compound **1** and 1,919,127 to compound **16**, respectively. Copies of this information could be obtained free of charge on application to CCDC, 12 Union Road, Cambridge CB2 1EZ, UK (fax: 44 1223 336 033; e-mail: deposit@ccdc.cam.ac.uk or http://www.ccdc.cam.ac.uk).

2.5. Physical measurements

Analytical data were obtained in a Fisons–Carlo Erba EA 1108 elemental micro-analyser. Infrared spectra were recorded by using KBr pellets on a Jasco FT-IR 6300 spectrometer. TG analysis (pyrolysis) of the studied compounds (295–800 °C) were carried out in air flow (100 mL/min) by a Shimadzu Thermobalance TGA–DTG–50H instrument, and a series of FT-IR spectra (20–30 per sample) of evolved gasses were recorded for the studied compounds using a coupled FT-IR Nicolet Magma 550 spectrometer. Electronic (diffuse reflectance) spectra were obtained in a Varian Cary-5E spectrophotometer.

3. Results and discussion

3.1. Compounds with 1-methyladenine

The introduction of an electron donating group at N1 in adenine is not expected to significantly change the basicity order of the N-heterocyclic donors. For instance, N9 > N7 > N3 is the proton affinity suggested for 1Meade. Compound **3** exhibits the H(N9)Meade$^+$ ion. As expected, the proton is located at N9, the most basic donor, in line with previously reported 1Meade salts [39]. Since N9 is no longer available, 1MeadeH binds the copper(II) ion via N7 and this metal binding pattern is assisted by an intramolecular H-bond involving the exocyclic amino group N6-H···O(carbox., 2.730(2) Å, 169.5°). This molecular

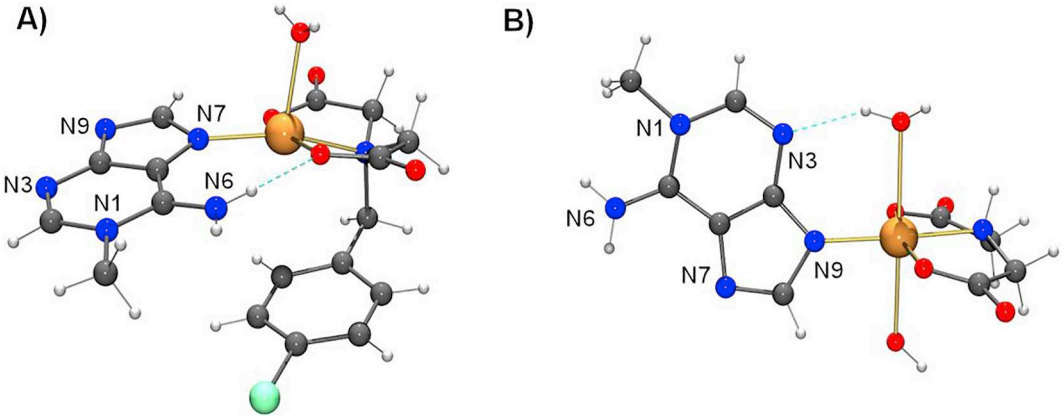

Fig. 1. Two different molecular recognition patterns for 1-methyladenine shown in the complex molecules of compounds (**2**) *[Cu(CBIDA)(1Meade)(H$_2$O)]·3H$_2$O* (**A**) and (**1**) *[Cu(IDA)(1Meade)(H$_2$O)$_2$]·4H$_2$O* (**B**), non-coordinated water molecules have been omitted for clarity. Intra-molecular H-bonds are depicted as cyan dotted lines. (For interpretation of the references to colour in this figure legend, the reader is referred to the web version of this article.)

recognition pattern is related to that of 1-methyladenosine, where N9 is also blocked (in such case by the pentose sugar), thus leading to metalation on the Hoogsteen face (N7), along with the referred intra-molecular H-bond [48]. Even if N9 is the most basic among donor atoms of 1Meade, the presence of the exocyclic amino group in position 6 could drive specific metal binding through N7 due to the possibility of reinforcing the metal-N7 coordination bond with an interligand H-bonding interaction. In fact, the same molecular recognition as compound **3** is observed for the neutral 1Meade ligand in compound **2** (Fig. 1A). Herein, 1Meade coordinates to the Cu(II) centre by N7, with the Cu—N7 bond being reinforced by an intra-molecular interligand H-bonding interaction type N6-H···O(carbox., 2.848(2) Å, 153.2°). In the former and the latter case, the metal centre exhibits a vaguely distorted 4 + 1 coordination polyhedron where the IDA-like chelating ligand exhibits a *mer*-NO$_2$ conformation, providing three donor atoms (N,O,O) to the metal surrounding while apical ligands are the chloride ion (**3**) or an aqua ligand (**2**), respectively. Another peculiarity that both structures share is the twist of 1Meade with regard to mean basal plane, which is related to the role of the N6(1Meade) exocyclic amino group in the crystal packing, which takes part of both intra- and inter-molecular H-bonds (Tables S2.3 and S3.3). In contrast, compound **1** (Fig. 1B), exhibits a distorted octahedral polyhedron (type 4 + 1 + 1, Table S1.2) and the binding pattern is via N9, the most basic donor. In this compound, IDA chelating ligand also exhibits a *mer*-NO$_2$ conformation while two aqua ligands are occupying the apical/distal sites. Interestingly, the 1Meade moiety is almost perpendicular to the mean Cu(II) basal plane in order to favour the formation of an intra-molecular H-bond that cooperates with that M-N9 bond, with one of the apical aqua ligands acting as H-donor (O—H···N3(1Meade), 2.762(3) Å, 146.3°). The characterization of the M-N9 + O—H···N3 and the M-N7 + N6-H···O evidence that metal binding is not only determined by the basicity of the N-donor but also by the possibility of reinforcing the M-N (purine) bond by weak interactions such as H-bonds.

Regarding crystal engineering, in compound **1**, the exocyclic amino group of 1Meade is only involved in intermolecular H-bonds, connecting adjacent complex molecules along the *a* axis. Moreover, weak massive head-to-tail π,π-stacking interactions between adjacent complex molecules, involving both rings of 1Meade ligands, contribute to the stabilization of the crystal ($d_{centroid\text{-}centroid}$ = 3.6066(2) Å, α = 1.52(2)°, β = 20.9° and γ = 21.6°). Self-assembly of 1Meade moieties is also observed in the crystal packing of compound **3**, but this time by the presence of symmetrical non-canonical H-bonds C2-H···N3 (3.156 Å, 121.63°). To the best of our knowledge, this kind of interaction have not been reported yet in DNA or RNA, although could be an alternative self-assembling motif to be considered for future non-canonical structures. For instance, this self-assembling arrangement has been recently claimed in a structural report of bis(adeninium) bis(hydrogensulfate) sulfate [49]. It should be noted that, when carefully analysed other crystal structures in the CSD database containing purine derivatives, this pattern has also been observed, not considered though [50–53]. Moreover, π,π-stacking interactions that involve the 6-membered ring of the 1Meade ligand and the *N*-naphthyl-moiety of the IDA-like chelating ligand ($d_{centroid\text{-}centroid}$ = 3.5035(2) Å, α = 3.88(14)°, β = 20.2° and γ = 17.6°) contribute to the stabilization of the 3D structure within the crystal (Fig. S3.4).

3.2. Compounds with 3-methyladenine

A total of six ternary compounds (**4–9**) have been isolated with different IDA-like chelators and 3Meade. Regardless of the substituents on the IDA skeleton, all compounds follow the same molecular recognition pattern that consists in a Cu—N7 coordination bond assisted by an intra-molecular interligand H-bonding interaction involving the exocyclic amino group [N6-H···O(carbox.)] (Fig. 2, see S4–S9). Compounds **5–8** have molecular nature and exhibit the general formula *[Cu(IDA-like)(3Meade)(H$_2$O)]·nH$_2$O* just differing in the amount of solvent molecules. In these cases, the Cu(II) centers show a 4 + 1 coordination polyhedron where the four closest donor atoms correspond to the tridentate IDA-like chelator in *mer*-conformation and the N7 atom from 3Meade, while the apical position is occupied by an aqua ligand. A similar Cu(II) environment is observed for compound **9** except for the apical position, which is occupied by an O-carboxylate atom. Indeed, it is the *syn-anti* carboxylate bridging role of CBIDA ligand which determines the polymeric nature of compound **9** (Fig. 3).

In line with compound **1**, compound **4** (Fig. 2), also exhibits an octahedral coordination polyhedron, type 4 + 1 + 1. However, in **4**,

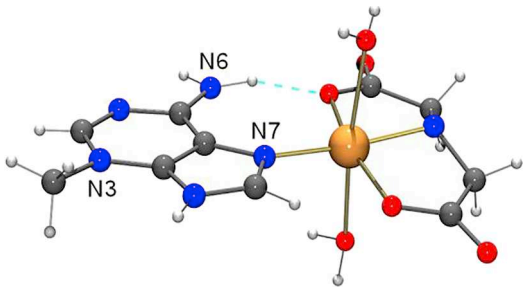

Fig. 2. Asymmetric unit of the crystal *[Cu(IDA)(3Meade)(H$_2$O)$_2$]·3H$_2$O* (**4**). Non-coordinated water molecules have been omitted for clarity. Intra-molecular H-bond is depicted as cyan dotted lines. (For interpretation of the references to colour in this figure legend, the reader is referred to the web version of this article.)

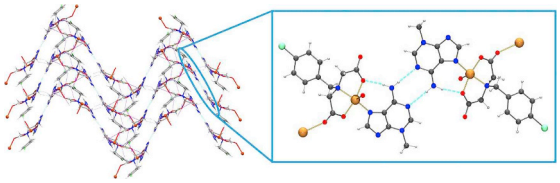

Fig. 3. 2D zig-zag layers in the crystal packing of *{[Cu(CBIDA)(3Meade)]·H_2O}$_n$* (**9**). Detail of two adjacent polymeric chains linked by reciprocal 3Meade [N6-H···N1] H-bonds is given. H-bonds are depicted as dashed cyan lines. Other hydrophobic interactions in the crystal network are depicted as dotted lines. (For interpretation of the references to colour in this figure legend, the reader is referred to the web version of this article.)

molecular recognition pattern does not change and remains faithful to the aforementioned 3Meade compounds. Again, IDA chelator adopts a *mer*-NO_2 conformation and metal binding consists in a Cu—N7 bond plus the intramolecular H-bond N6-H···O(carbox., 2.720(6) Å, 161.9°). The observed molecular recognition pattern is in line with previous results [32,34–36]. Besides the difference in basicity, why N9 or N1 of 3Meade are not involved in coordination in any of the reported complexes can be understood considering the significant steric hindrance that the methyl group in N3 imposes over N9 and the N6-exocylic amino group exerts on N1.

Regarding the crystal architecture, it should be remarked that all compounds (**4–9**) involve the exocyclic amino group both in intra- and in intermolecular H-bonding interactions which leads to mild torsion of the 3Meade moiety regarding the Cu(II) mean basal plane (dihedral angles between 10 and 35°). Compounds **4–8** connect adjacent complex molecules using two H-bonds through the Watson-Crick edge of the nucleobase moiety, with N6—H acting as H-donor [N6-H···O(carboxylate or aqua)] and N1(3Meade) acting as H-acceptor [O-H(aqua)···N1(3Meade)]. In contrast, compound **9** exhibits reciprocal canonical Watson-Crick H-bonds between two adjacent 3Meade ligands N6-H···N1(3Meade) H-bonds yielding 2D layers of the polymer that connect to each other via hydrophobic interactions benzyl-chloride (Fig. 3).

3.3. Compounds with 7-methyladenine

Only one compound, namely compound **10**, was successfully isolated after the reaction of different [Cu(IDA-like)] chelates and 7Meade. In compound **10**, Cu(II) coordination environment is very close to a regular square pyramidal coordination. The chelating ligand MIDA displays its three donor atoms adopting a *mer*-NO_2 conformation. The Cu(II) basal plane is then satisfied by the N3 donor of 7Meade, while the apical site is occupied by one aqua ligand (Fig. 4). Methylation on N7 was expected to drive metal coordination through N9, according to the basicity order. Indeed, only one Zn(II) metal complex of neutral 7Meade has been reported in the literature [27] where the Zn—N9 bond is observed. However, in compound **10**, coordination involves the less basic of the N-heterocyclic donor atoms in the purine moiety instead. If we look only to the asymmetric unit of this crystal, molecular recognition via N3 seems surprising. This pattern does not allow any cooperation between the coordination bond and an intramolecular interligand interaction because (i) there is no tautomerizable proton in neutral 7Meade and (ii) the chelating ligand methyl-iminodiacetate only offers H-acceptors (O-carboxylate atoms) as terminal groups. In fact, monodentate Cu—N3 coordination is striking even for neutral adenine, where only 7 crystal structures have been reported with this metal binding pattern [40,42,54,55]. More common is to observe N3 involved in bridging roles in polynuclear complexes [56–60], as well as in N9-tethered adenine ligands, where a multidentate ligand conjugation strategy is followed [61,62].

Interestingly, in compound **10**, 7Meade moiety is nearly perpendicular to the mean basal coordination plane, with the dihedral angle being almost 80°. This fact is certainly influenced by the presence of further weak interactions in the crystal. For instance, the two H-atoms of the exocyclic amino group are involved in intermolecular H-bonds, acting as H-donors, and building 1D chains that extend along the *a* axis, which are further stabilized by weak but massive π,π-stacking interactions among adjacent antiparallel 7Meade moieties ($d_{centroid\text{-}centroid}$ = 3.657(3) Å, α = 0(2)°, β = 25.1° and γ = 25.1° and ($d_{centroid\text{-}centroid}$ = 3.539(2) Å, α = 0.85(2)°, β = 20.6° and γ = 21.2°) (Fig. 4). Non-canonical C8-H···N1 hydrogen bonds (3.404(6) Å, 176.4°) play a key role in the molecular recognition, joining adjacent chains and building infinite 2D motifs, Additional intermolecular H-bonds involving non-coordinated water molecules (Table S10.3), such as O2-H···N9(3Meade), complete the 3D framework (Fig. S10.4).

3.4. Compounds with 9-methyladenine

The largest structural information on N-substituted adenines is devoted to N9-substitutions due to its proximity with natural nucleosides. In this context, mononuclear metal binding to N7 is the most frequently observed pattern, even in adenosine ligands, and thereby the one to be expected [17,18,63,64]. A total of 6 compounds (**11–16**) were characterized with IDA-like chelators and 9Meade. Compound **11**, has a molecular nature and, as previously described for compounds **1** and **4** (also with the IDA chelator), exhibits a 4 + 1 + 1 coordination polyhedron. In this case, one of the aqua-distal bonds is rather long (2.881(4) Å), therefore one might consider it just a contact, since the sum of the Van der Waals radii is 2.90 Å (Cu 1.40 Å + O 1.50 Å). Compounds **14–16**, which involve *N*-benzyl-IDA-like chelators, are also molecular but Cu(II) environment is defined as a distorted square-base pyramidal coordination instead. In contrast, compounds **12–13**, with *N*-alkyl-IDA chelators, have a polymeric nature. These latter complexes essentially differ in the Cu(II) environment, compound **12** exhibits a 4 + 1 + 1 coordination while compound **13** shows a 4 + 1 coordination, and in the bridging role of the IDA carboxylate ligands, with MIDA building the coordination polymer by an *anti-anti* role while EIDA exhibits a *syn-anti* role. In all reported complexes, regardless of the N-IDA substituent or the molecular or polymeric nature of the above referred complexes, the metal-N7 molecular recognition pattern is always observed along with the corresponding intra-molecular interligand H-bonding interaction involving the exocyclic amino group N6-H···O (carboxylate IDA) (Fig. 5B). The sole exception can be attributed to compound **11**, where the intra-molecular H-bond N(36)-H(36A)···O21(coord. Carboxylate, 3.330(5) Å, 140.2°) might not be considered as an effective intra-molecular interaction due to its length but the N(36)-H(36A)···O1(aqua apical, 3.076(5) Å, 113.4°) interaction might be considered instead (Fig. 5A, Table S11.3).

A comprehensive view on the structure of compound **11** highlights the peculiar behavior of this compound. First, it should be reminded that this compound could be considered at the interface between a distorted octahedron (4 + 1 + 1), as occurs for the IDA compounds **1** and **4**, and a squared-based pyramidal coordination, since one of the Cu-O(aqua) distal sites is almost the sum of the Van der Waals radii. This latter 4 + 1 coordination seems to promote the cooperation between the Cu—N7 bond and the intra-molecular interligand N6-H···O interaction in compounds **2**, **3**, **5–9** and **12–16** but in compound **11** only a residual contact is observed. This fact is also influenced by the involvement of the exocyclic amino group N6—H in two additional H-bonding interactions: the aforementioned intra-molecular H-bond, involving one apical aqua ligand, and one inter-molecular interaction [N(36)-H(36A)···O(22)#6, 3.146(5) Å, 139.3°, symmetry code #6-x + 2,-y + 1,-z + 1] (see table S11.3.). Besides the "trifurcated" role of the N6—H group, which certainly elongates the H-bonding distances within this group, the other N-heterocyclic atoms within the six member ring of the purine moiety (N1, N3) are also involved in intermolecular interligand H-bonds, contributing to the high value of the dihedral angle between the mean basal coordination plane and the 9Meade plane, close to 60°. Furthermore, intense infinite π,π-stacking interactions

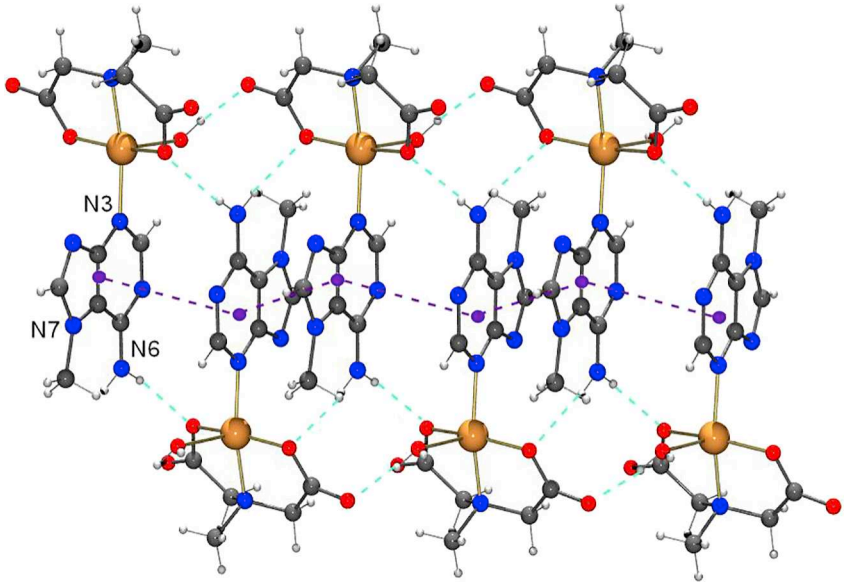

Fig. 4. 1D chains in the crystal of *[Cu(MIDA)(7Meade)(H_2O)]·4H_2O* (**10**). Metal binding pattern is via N3(7Meade). H-bonding network, involving the N6—H group and the apical aqua ligand, is depicted as dashed cyan lines. π,π-stacking interactions between 3Meade ligands are shown as dashed purple lines. Non-coordinated water molecules omitted for clarity. (For interpretation of the references to colour in this figure legend, the reader is referred to the web version of this article.)

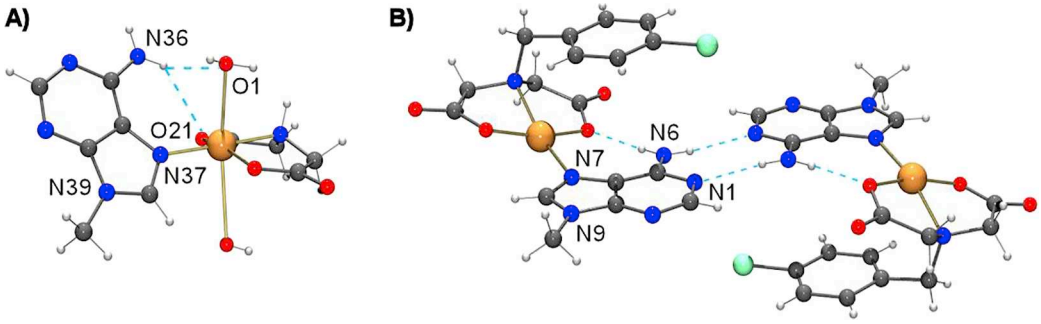

Fig. 5. A) Asymmetric unit in the compound *[Cu(IDA)(9Meade)(H_2O)$_2$]·3H_2O* (**11**). In the crystal, the N6—H exocyclic amino group is involved in a 'trifurcated' H-bond, with the intra-molecular N(36)-H(36A)···O(1) [3.076(5) Å, 113.4°] and N(36)-H(36A)···O(21) [3.330(5) Å, 140.2°] H-bonds being depicted in cyan dashed lines. The intermolecular H-bond involving the N(36)-H(36A) donor and solvent molecules have been omitted for clarity. B) Pairs of complex molecules in the crystal of compound (**16**) *[Cu(CBIDA)(9Meade)(H_2O)]·H_2O*. Symmetrically related intra- and inter-molecular H-bonding interactions [N6-H···O (2.782(3)Å, 167.6°) and N6-H···N1 (3.036(3)Å, 173.2°), respectively] are depicted in cyan. Non coordinated water molecules are omitted for clarity in this figure. (For interpretation of the references to colour in this figure legend, the reader is referred to the web version of this article.)

between the six membered rings of adjacent 9Meade ligands along the *a* axis ($d_{centroid\text{-}centroid}$ = 3.239(3) Å, α = 0°, β = 8.6° and γ = 8.6°) contribute to define the 3D architecture of the crystal.

The Cu-N7 + N6-H···O metal binding pattern was certainly expected, as previously discussed for the N7-coordination in 3Meade. Although in 9Meade the proton affinity is assumed to be N1 > N7 > N3, the N1 and the N3 donors are affected by the steric hindrance from the *orto*-N6-exocyclic amino group and the substituted-N9 moiety, respectively, so their metal binding is limited. The effect of the referred steric hindrance seems to be reduced provided the size of the metal ion increases. For instance, a structural search on N9-substituted adenine-like ligands only shows monodentate N1-coordination when bigger metal ions such as platinum(II) or silver(I) are present [65,66]. On the other hand, it should also be considered the fact that the M-N7 coordination allows the N6-amino group to be involved not only in intra-molecular H-bonding interactions, which cooperate with the M-N7 bond, but also to further stabilize the structure via inter-molecular H-bonds, for instance involving the Watson-Crick edge of the purine moiety (Fig. 5B).

4. Concluding remarks

The use of N1, N3 and N9-methyladenine in ternary complexes with different copper(II)-iminodiacetate-like chelates, remarks the relevance of the Cu-N7 + N6-H···O metal binding pattern. The preference for this molecular recognition pattern is certainly influenced by (i) the relatively high basicity of this N-donor, (ii) the lower steric hindrance of N7 compared to N1, N3 or N9 in the studied *N*-methyladenine ligands and (iii) the possibility of assisting the Cu—N bond with the corresponding intra-molecular H-bond. In this context, the cooperation of the H-bond seems to be promoted by the H-accepting role of the O-coordinated carboxylate atoms from the iminodiacetate-like ligands, in *mer*-NO_2 conformation, as well as the common elongated square-base pyramidal coordination, type 4 + 1, of all the reported compounds that exhibit the referred molecular recognition pattern. The only way to prevent the formation of the Cu—N7 bond in the studied compounds was either blocking it (using the 7Meade ligand) or favouring the formation of alternative intra-molecular H-bonds that could additionally assist the M-N(Meade) bond, without neglecting further inter-molecular interactions that provide stability to the crystal packing. Interestingly, in the ternary complex [Cu(IDA-like)(7Meade)], 7Meade binds the metal ion via the minor groove binder N3. This metal binding pattern for 7Meade is reported herein for the first time. The reasons why this particular complex prefers to coordinate the purine moiety by N3 instead of N9 still remains unclear, although packing forces, including stacking and hydrophobic interactions, might partially explain this behaviour.

Acknowledgements

Financial support from the Excellence Network "Metal Ions in

Biological Systems" MetalBio CTQ2017-90802-REDT (Plan Estatal de Investigación Científica y Técnica y de Innovación) and the Research group FQM-283 (Junta de Andalucía) is gratefully acknowledged.

Appendix A. Supplementary data

Supplementary data to this article can be found online at https://doi.org/10.1016/j.jinorgbio.2019.110801.

References

[1] B. Lippert, Multiplicity of metal ion binding patterns to nucleobases, Coord. Chem. Rev. 200–202 (2000) 487–516, https://doi.org/10.1016/S0010-8545(00)00260-5.
[2] A. Sigel, H. Sigel, R.K.O. Sigel (Eds.), Metal Ions in Life Science, Springer, 2012.
[3] K.D. Mjos, C. Orvig, Metallodrugs in medicinal inorganic chemistry, Chem. Rev. 114 (2014) 4540–4563, https://doi.org/10.1021/cr400460s.
[4] H. Cai, Y.-L. Huang, D. Li, Biological metal–organic frameworks: structures, host–guest chemistry and bio-applications, Coord. Chem. Rev. 378 (2019) 207–221, https://doi.org/10.1016/J.CCR.2017.12.003.
[5] J. Šebera, A. Dubankova, V. Sychrovský, D. Ruzek, E. Boura, R. Nencka, The structural model of Zika virus RNA-dependent RNA polymerase in complex with RNA for rational design of novel nucleotide inhibitors, Sci. Rep. 8 (2018) 11132, , https://doi.org/10.1038/s41598-018-29459-7.
[6] S. Medici, M. Peana, V.M. Nurchi, J.I. Lachowicz, G. Crisponi, M.A. Zoroddu, Noble metals in medicine: latest advances, Coord. Chem. Rev. 284 (2015) 329–350, https://doi.org/10.1016/J.CCR.2014.08.002.
[7] D.K. Patel, A. Domínguez-Martín, M. del P. Brandi-Blanco, D. Choquesillo-Lazarte, V.M. Nurchi, J. Niclós-Gutiérrez, Metal ion binding modes of hypoxanthine and xanthine versus the versatile behaviour of adenine, Coord. Chem. Rev. 256 (2012) 193–211, https://doi.org/10.1016/J.CCR.2011.05.014.
[8] R.F. Stewart, L.H. Jensen, Crystal structure of 9-Methyladenine, J. Chem. Phys. 40 (1964) 2071–2075, https://doi.org/10.1063/1.1725475.
[9] K.N. Jarzembska, A.M. Goral, R. Gajda, P.M. Dominiak, Hoogsteen–Watson–Crick 9-methyladenine:1-methylthymine complex: charge density study in the context of crystal engineering and nucleic acid base pairing, Cryst. Growth Des. 13 (2013) 239–254, https://doi.org/10.1021/cg301393e.
[10] A. Gaballa, H. Schmidt, G. Hempel, D. Reichert, C. Wagner, E. Rusanov, D. Steinborn, Protonated nucleobase ligands: synthesis, structure and characterization of 9-methyladeninium hexachloroplatinate and pentachloro(9-methyladeninium)platinum(IV), J. Inorg. Biochem. 98 (2004) 439–446, https://doi.org/10.1016/J.JINORGBIO.2003.12.005.
[11] K. Aoki, M.A. Salam, Interligand interactions affecting specific metal bonding to nucleic acid bases. A case of [Rh2(OAc)4], [Rh2(HNOCCF3)4], and [Rh2(OAc)2(HNOCCF3)2] toward purine nucleobases and nucleosides, Inorganica Chim. Acta. 339 (2002) 427–437, https://doi.org/10.1016/S0020-1693(02)01042-3.
[12] R.F. Bryan, K.-I. Tomita, The crystal structures of salts of methylated purines and pyrimidines. II. 9-Methyladenine dihydrobromide, Acta Crystallogr. 15 (1962) 1179–1182, https://doi.org/10.1107/S0365110X62003060.
[13] W. Saettger, D. Suck, Base pairing of a transfer RNA minor constituent: geometry of the 1-methyl-4-thiouracil · 9-methyladenine base pair, J. Mol. Biol. 60 (1971) 87–99, https://doi.org/10.1016/0022-2836(71)90449-9.
[14] M.N. Frey, T.F. Koetzle, M.S. Lehmann, W.C. Hamilton, Precision neutron diffraction structure determination of protein and nucleic acid components. XII. A study of hydrogen bonding in the purine-pyrimidine base pair 9-methyladenine · 1-methylthymine, J. Chem. Phys. 59 (1973) 915–924, https://doi.org/10.1063/1.1680114.
[15] E. Sletten, M. Ruud, Crystallographic studies on metal{−-}nucleotide base complexes. V. Tetraaquo-bis-(9-methyladenine)-copper(II) dichloride dihydrate, Acta Crystallogr. Sect. B. 31 (1975) 982–985, https://doi.org/10.1107/S0567740875004335.
[16] E.A.H. Griffith, N.G. Charles, E.L. Amma, Structure of the adduct of dimethyl sulfoxide and 9-methyladenine with cadmium chloride [catena-di-mu-chloro-(dimethyl sulfoxide) (9-methyladenine)cadmium(II)], Acta Crystallogr. Sect. B. 38 (1982) 942–944, https://doi.org/10.1107/S0567740882004518.
[17] A. Egger, V.B. Arion, E. Reisner, B. Cebrián-Losantos, S. Shova, G. Trettenhahn, B.K. Keppler, Reactions of potent antitumor complex trans-[RuIIICl4(indazole)2]- with a DNA-relevant nucleobase and thioethers: insight into biological action, Inorg. Chem. 44 (2005) 122–132, https://doi.org/10.1021/ic048967h.
[18] S. Ibáñez, M. Béla, P.J. Sanz Miguel, D. Steinborn, I. Pretzer, W. Hiller, B. Lippert, The challenge of deciphering linkage isomers in mixtures of oligomeric complexes derived from 9-Methyladenine and trans-(NH3)2PtII units, Chem. A Eur. J. 21 (2015) 5794–5806, https://doi.org/10.1002/chem.201406378.
[19] J. Thomas-Gipson, G. Beobide, O. Castillo, A. Luque, J. Pascual-Colino, S. Pérez-Yáñez, P. Román, Providing evidence for the requirements to achieve supramolecular materials based on metal–nucleobase entities, CrystEngComm 20 (2018) 2528–2539, https://doi.org/10.1039/C8CE00141C.
[20] M.J. Olivier, A.L. Beauchamp, Metal binding to N(1) of 9-methyladenine in the 1:1 complex with methylmercuric nitrate, Inorg. Chem. 19 (1980) 1064–1067, https://doi.org/10.1021/ic50206a057.
[21] F. Schwarz, B. Lippert, H. Schöllhorn, U. Thewalt, Mono-, di- and trinuclear Pt(II), mononuclear Pt(IV), mixed Pt(II),Pt(IV), mixed Pt(II),Ag(I) complexes of 9-methyladenine (9-MeA), and the X-ray structure of [(dien)Pt(9-MeA-N1)](NO3)2·H2O, Inorganica Chim. Acta. 176 (1990) 113–121, https://doi.org/10.1016/S0020-1693(00)85101-4.
[22] J. Viljanen, K.D. Klika, R. Sillanpää, J. Arpalahti, Intramolecular migration of coordinated platinum(II) from the N7 site to the exocyclic amino group in 9-methyladenine, Inorg. Chem. 38 (1999) 4924–4925, https://doi.org/10.1021/ic990498+.
[23] N. Shan, S.J. Vickers, H. Adams, M.D. Ward, J.A. Thomas, Switchable electron-transfer processes in a mixed-valence, kinetically locked, trinuclear RuII metallamacrocycle, Angew. Chemie Int. Ed. 43 (2004) 3938–3941, https://doi.org/10.1002/anie.200460022.
[24] M.S. Lüth, G. Kampf, M. Garijo Anorbe, R. Griesser, B.P. Operschall, H. Sigel, B. Lippert, Connectivity patterns and rotamer states of nucleobases determine acid–base properties of metalated purine quartets, J. Inorg. Biochem. 148 (2015) 93–104, https://doi.org/10.1016/J.JINORGBIO.2015.02.004.
[25] F.M. Albertí, T. Mihály, B. Lippert, P.J.S. Miguel, Unsupported single-walled water cluster nanotube: a novel hydrogen bonding pattern for water organization, CrystEngComm 14 (2012) 6178–6181, https://doi.org/10.1039/C2CE25647A.
[26] T.J. Kistenmacher, T. Shigematsu, Structural chemistry of N(7)-substituted purines: 7-methyladenine dihydrochloride, Acta Crystallogr. Sect. B. 31 (1975) 211–217, https://doi.org/10.1107/S0567740875002373.
[27] C.L. Price, M.R. Taylor, 7-Methyl-3-adeninium Trichloro(7-methyladenine)trichlorozinc(II) monohydrate, Acta Crystallogr. Sect. C. 52 (1996) 2736–2738, https://doi.org/10.1107/S0108270196009079.
[28] R. Marek, A. Křístková, K. Maliňáková, J. Toušek, J. Marek, M. Hocek, O.L. Malkina, V.G. Malkin, Interpretation of indirect nuclear spin − spin couplings in isomers of adenine: novel approach to analyze coupling Electron deformation density using localized molecular orbitals, J. Phys. Chem. A 114 (2010) 6689–6700, https://doi.org/10.1021/jp102186r.
[29] C.S. Petersen, S. Furberg, Crystal structure of 3-Ethyladenine, Acta Chem. Scand. B29 (1975) 37–40, https://doi.org/10.3891/acta.chem.scand.29b-0037.
[30] Y. Yamagata, K.-i. Tomita, Structure of 3-methyladenine hydrochloride, Acta Crystallogr. Sect. C. 43 (1987) 1195–1197, https://doi.org/10.1107/S0108270187092540.
[31] Y. Yamagata, M. Kato, S. Fujii, Model for a recognition of 3-methyladenine by 3-methyladenine DNA glycosylase: the stacking interaction between 3-methyladenine and indole rings, Chem. Pharm. Bull. (Tokyo). 42 (1994) 2385–2387, https://doi.org/10.1248/cpb.42.2385.
[32] J.D. Orbell, C. Solorzano, L.G. Marzilli, T.J. Kistenmacher, Coordinating properties of alkylated 6-aminopurines. Electrostatic potential distributions for 3-methyladenine and 9-methyladenine and preparation and structure of cis-diamminebis(3-methyladenine)platinum(II) nitrate trihydrate, Inorg. Chem. 21 (1982) 2630–2636, https://doi.org/10.1021/ic00137a020.
[33] W.S. Sheldrick, P. Gross, Preparation and structural characterization of methylmercury(II) complexes of 3-methyladenine, Inorganica Chim. Acta. 156 (1989) 139–144, https://doi.org/10.1016/S0020-1693(00)90379-7.
[34] A. Hazell, J. Ouyang, L.E. Khoo, Dichlorodimethylbis(3-methyladenine)dimethyltin(IV), Acta Crystallogr. Sect. C. 53 (1997) 406–408, https://doi.org/10.1107/S0108270196015132.
[35] S. Pérez-Yáñez, O. Castillo, J. Cepeda, J.P. García-Terán, A. Luque, P. Román, Supramolecular architectures of metal–oxalato complexes containing purine nucleobases, Inorganica Chim. Acta. 365 (2011) 211–219, https://doi.org/10.1016/J.ICA.2010.09.012.
[36] S. Pérez-Yáñez, G. Beobide, O. Castillo, J. Cepeda, A. Luque, P. Román, Directing the formation of adenine coordination polymers from tunable copper(II)/Dicarboxylato/adenine paddle-wheel building units, Cryst. Growth Des. 12 (2012) 3324–3334, https://doi.org/10.1021/cg300446d.
[37] A. García-Raso, J.J. Fiol, A. Tasada, F.M. Albertí, F. Bádenas, X. Solans, M. Font-Bardia, N9,N9′-polymethylene-bisadenine complexes with d10 metal ions, Polyhedron 26 (2007) 949–957, https://doi.org/10.1016/J.POLY.2006.09.074.
[38] A.T.H. Lenstra, E.N. Duesler, B. Golankiewicz, Structure of 1-(2-isopentenyl)adenine, Acta Crystallogr. Sect. B. 37 (1981) 296–298, https://doi.org/10.1107/S0567740881002859.
[39] W.S. Sheldrick, G. Heeb, Preparation and structural characterization of methylmercury(II) complexes of the minor tRNA-base 1-methyladenine, Inorganica Chim. Acta. 194 (1992) 67–73, https://doi.org/10.1016/S0020-1693(00)85824-7.
[40] E. Bugella-Altamirano, D. Choquesillo-Lazarte, J. González-Pérez, M. Sánchez-Moreno, R. Marin-Sánchez, J. Martin-Ramos, B. Covelo, R. Carballo, A. Castiñeiras, J. Niclós-Gutiérrez, Three new modes of adenine-copper(II) coordination: interligand interactions controlling the selective N3-, N7- and bridging μ-N3,N7-metal-bonding of adenine to different N-substituted iminodiacetato-copper(II) chelates, Inorganica Chim. Acta 339 (2002) 160–170, https://doi.org/10.1016/S0020-1693(02)00920-9.
[41] H. El Bakkali, New Copper(II) Chelates with Nitrogenated Heterocycles as Co.Ligands: A Structural Study (PhD), University of Granada, 2013.
[42] M.J. Sánchez-Moreno, D. Choquesillo-Lazarte, J.M. González-Pérez, R. Carballo, A. Castiñeiras, J. Niclós-Gutiérrez, Inter-ligand interactions and the selective formation of the unusual metal–N3(adenine) bond in ternary copper(II) complexes with N-benzyliminodiacetato(2−) ligands, Inorg. Chem. Commun. 5 (2002) 800–802, https://doi.org/10.1016/S1387-7003(02)00559-2.
[43] BRUKER, APEX2 Software, (2010).
[44] G.M. Sheldrick, SADABS. Program for Empirical Absorption Correction of Area Detector Data, (2009).
[45] G.M. Sheldrick, A short history of SHELX, Acta Crystallogr. Sect. A. 64 (2008) 112–122, https://doi.org/10.1107/S0108767307043930.
[46] A.L. Spek, PLATON. A Multipurpose Crystallographic Tool, (2010).
[47] C.F. Macrae, I.J. Bruno, J.A. Chisholm, P.R. Edgington, P. McCabe, E. Pidcock,

L. Rodriguez-Monge, R. Taylor, J. van de Streek, P.A. Wood, Mercury CSD 2.0 - new features for the visualization and investigation of crystal structures, J. Appl. Crystallogr. 41 (2008) 466–470, https://doi.org/10.1107/S0021889807067908.
[48] J.R. Rubin, T.P. Haromy, M. Sundaralingam, Structure of the anti-cancer drug complex tetrakis(mu-acetato)-bis(1-methyladenosine)dirhodium(II) monohydrate, Acta Crystallogr. Sect. C. 47 (1991) 1712–1714, https://doi.org/10.1107/S010827019100032X.
[49] F. Guenifa, L. Bendjeddou, A. Cherouana, S. Dahaoui, C. Lecomte, Bis(adeninium) bis(hydrogensulfate) sulfate, Acta Crystallogr. Sect. E. 68 (2012) o3266–o3267, https://doi.org/10.1107/S1600536812044728.
[50] G. Bunick, D. Voet, The structure of 9-[3-(3-indolyl)-propyl]adenine. A model for protein/nucleic acid interactions, Acta Crystallogr. Sect. B. 38 (1982) 575–580, https://doi.org/10.1107/S0567740882003409.
[51] S. Ikonen, A. Valkonen, E. Kolehmainen, X-ray structures of five variably tert-butoxycarbonyl-substituted adenines and their liquid and solid state NMR investigations, J. Mol. Struct. 930 (2009) 147–156, https://doi.org/10.1016/J.MOLSTRUC.2009.05.006.
[52] W.-X. Zhang, T. Shiga, H. Miyasaka, M. Yamashita, New approach for designing single-chain magnets: Organization of Chains via hydrogen bonding between nucleobases, J. Am. Chem. Soc. 134 (2012) 6908–6911, https://doi.org/10.1021/ja300152k.
[53] I. Sinha, A. Hepp, J. Kösters, J. Müller, Metal complexes of 6-pyrazolylpurine derivatives as models for metal-mediated base pairs, J. Inorg. Biochem. 153 (2015) 355–360, https://doi.org/10.1016/J.JINORGBIO.2015.07.002.
[54] J.E. Kickham, S.J. Loeb, S.L. Murphy, Molecular receptors for adenine and guanine employing metal coordination, hydrogen-bonding and π-stacking interactions, Chem. – A Eur. J. 3 (1997) 1203–1213, https://doi.org/10.1002/chem.19970030807.
[55] J.P. García-Terán, O. Castillo, A. Luque, U. García-Couceiro, P. Román, F. Lloret, One-dimensional oxalato-bridged Cu(II), Co(II), and Zn(II) complexes with purine and adenine as terminal ligands, Inorg. Chem. 43 (2004) 5761–5770, https://doi.org/10.1021/ic049569h.
[56] J. Cepeda, O. Castillo, J.P. García-Terán, A. Luque, S. Pérez-Yáñez, P. Román, Supramolecular architectures and magnetic properties of self-assembled windmill-like dinuclear copper(II) complexes with purine ligands, Eur. J. Inorg. Chem. 2009 (2009) 2344–2353, https://doi.org/10.1002/ejic.200900090.
[57] M. del Pilar Brandi-Blanco, D. Choquesillo-Lazarte, A. Domínguez-Martín, A. Matilla-Hernández, J.M. González-Pérez, A. Castiñeiras, J. Niclós-Gutiérrez, Molecular recognition modes between adenine or adeniniun(1 +) ion and binary MII(pdc) chelates (MCoZn; pdc = pyridine-2,6-dicarboxylate(2-) ion), J. Inorg. Biochem. 127 (2013) 211–219, https://doi.org/10.1016/J.JINORGBIO.2013.06.008.
[58] C.S. Purohit, A.K. Mishra, S. Verma, Four-stranded coordination helices containing silver−adenine (purine) metallaquartets, Inorg. Chem. 46 (2007) 8493–8495, https://doi.org/10.1021/ic701465d.
[59] H.-F. Ma, L.-W. Ding, L. Chen, Y.-L. Wang, Q.-Y. Liu, Two cadmium compounds with adenine and carboxylate ligands: syntheses, structures and photoluminescence, J. Coord. Chem. 70 (2017) 145–155, https://doi.org/10.1080/00958972.2016.1256477.
[60] Á. Valentín-Pérez, J. Perles, S. Herrero, R. Jiménez-Aparicio, Coordination capacity of cytosine, adenine and derivatives towards open-paddlewheel diruthenium compounds, J. Inorg. Biochem. 187 (2018) 109–115, https://doi.org/10.1016/J.JINORGBIO.2018.06.010.
[61] C. Price, M.R.J. Elsegood, W. Clegg, A. Houlton, Directed metallation of adenine-N3via nucleobase–ligand conjugation, J. Chem. Soc. Chem. Commun. (1995) 2285–2286, https://doi.org/10.1039/C39950002285.
[62] D. Amantia, C. Price, M.A. Shipman, M.R.J. Elsegood, W. Clegg, A. Houlton, Minor groove site coordination of adenine by platinum group metal ions: effects on basicity, base pairing, and electronic structure, Inorg. Chem. 42 (2003) 3047–3056, https://doi.org/10.1021/ic020657g.
[63] M. Mikola, K.D. Klika, J. Arpalahti, The kinetics of substitution reactions of mixed platinum(II)–Bis(nucleoside) complexes in aqueous solution in the presence of Thiourea; X-ray crystal structure determination of cis-[Pt(NH3)2(adenosine-N7)2](ClO4)2·3.5H2O, Chem. – A Eur. J. 6 (2000) 3404–3413, https://doi.org/10.1002/1521-3765(20000915)6:18<3404::AID-CHEM3404>3.0.CO;2-R.
[64] A.D. Collins, P. De Meester, D.M.L. Goodgame, A.C. Skapski, The site of metal ion binding in a nickel derivative of adenosine 5′-monophosphate: an X-ray study, Biochim. Biophys. Acta - Nucleic Acids Protein Synth. 402 (1975) 1–6, https://doi.org/10.1016/0005-2787(75)90363-9.
[65] A.K. Mishra, R.K. Prajapati, S. Verma, Probing structural consequences of N9-alkylation in silver-adenine frameworks, Dalt. Trans. 39 (2010) 10034–10037, https://doi.org/10.1039/C0DT00557F.
[66] I.A. Riddell, T.C. Johnstone, G.Y. Park, S.J. Lippard, Nucleotide binding preference of the Monofunctional platinum anticancer-agent Phenanthriplatin, Chem. – A Eur. J. 22 (2016) 7574–7581, https://doi.org/10.1002/chem.201600236.